ITERATIVE TARGET DETECTION APPROACH FOR THROUGH-THE-WALL RADAR IMAGING

Christian Debes[1], *Jesper Riedler*[1], *Moeness G. Amin*[2] *and Abdelhak M. Zoubir*[1]

[1]Signal Processing Group
Technische Universität Darmstadt
Darmstadt, Germany

[2]Center for Advanced Communications
Villanova University
Villanova, PA, USA

ABSTRACT

We consider the problem of target detection in Through-the-wall Radar Imaging when no a priori knowledge about the image statistics is available. An iterative approach which adapts itself to the unknown image statistics and thus allows for automatic target detection is presented. Two variants, based on 2D median filtering and morphological operations, are described in details. The proposed detection schemes are tested using experimental data, considering the problem of 3D reconstruction of a scene hidden behind a concrete wall.

Index Terms— Through-the-wall, radar imaging, image fusion, morphological image processing

1. INTRODUCTION

"Seeing" through walls or other visually opaque materials is of high practical interest in numerous civilian, law enforcement and military scenarios [1, 2, 3]. Through-the-Wall (TTW) Radar Imaging is a technique using electromagnetic waves below the S-band to penetrate e.g. a wall and illuminate an indoor scene. Electromagnetic waves encounter significant attenuation, phase distortions and severe multipath propagation effects as they make a round-trip propagation through walls and reflect from targets with various radar cross sections (RCS). The radar image statistics for indoor applications are different compared to those from 'classical' radar scenarios, e.g. in naval or air traffic applications where radar waves are often only disturbed by electronic noise.
In order to achieve high cross-range and range imaging resolution large array apertures and large signal bandwidths are needed. Due to the presence of the wall and the high variety of indoor settings and types of possible targets (e.g. humans, weapons, explosives, typical room items such as chairs, tables or cabinets) the image statistics, when applying delay and sum beamforming, vary dramatically depending on the (unknown) scene within the enclosed structure. Any practical TTW radar imaging system should, therefore, provide self-learning procedures, yielding acceptable target detection results without assuming a priori knowledge of the image statistics.

The work by Moeness Amin is supported by ONR, grant no N00014-07-C-0413

2. DETECTION SCHEMES IN THROUGH-THE-WALL RADAR IMAGING

Let the hidden 3D scene be accurately representable by a finite set of voxels $B(i,j,h)$ with $0 \leq i < I$, $0 \leq j < J$ and $0 \leq h < H$ as shown in Figure 1. Each voxel $B(i,j,h)$ can take the values '0' or '1' representing the absence or presence of a target at position (i,j,h), respectively.
The 3D scene is now illuminated by using a set of K TTW radar systems, placed at different vantage points. If access to only one wall is possible, the K radar systems can be placed along the same wall, possibly at different standoff positions. If access to more than one wall is possible, one can make use of neighboring walls to illuminate the scene from different viewing angles. Multiple-viewing is of special importance when targets of interest are not visible from all vantage points.

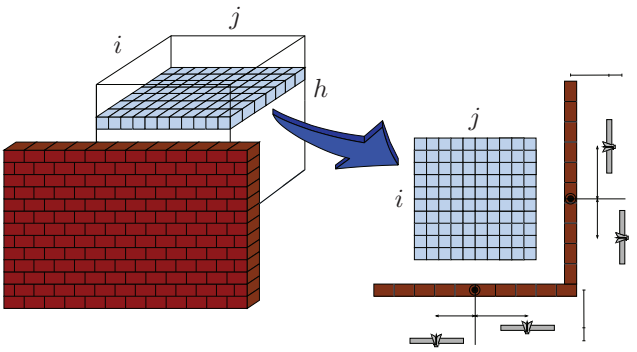

Fig. 1. Through-the-wall Radar Imaging: Setup

The total set of acquired 3D TTW radar images is denoted as $\{Y_k(i,j,h)\}_{k=1}^{K}$. The aim of a target detection scheme is to estimate $B(i,j,h)$ from $\{Y_k(i,j,h)\}_{k=1}^{K}$. A statistically meaningful way to fuse and binarize $\{Y_k(i,j,h)\}_{k=1}^{K}$ is to use likelihood ratio tests. We use a simple signal model:

$$Y_k(i,j,h) = \eta \cdot s(i,j,h) + u_k(i,j,h) \qquad (1)$$

where $s(i,j,h)$ describes the signal contribution and $u_k(i,j,h)$ represents the noise contribution when illuminating the voxel (i,j,h) from the k-th vantage point. We can then define the null and alternative hypothesis as

$$H_0: \quad \eta = 0; \quad H_1: \quad \eta > 0 \tag{2}$$

Given the conditional probability density functions (pdf's) $p(Y_k(i,j,h)|H_0)$ and $p(Y_k(i,j,h)|H_1)$, one can formulate the likelihood ratio test (LRT) as $\mathrm{LR}(i,j,h) = \prod_{k=1}^{K} \frac{p(Y_k(i,j,h)|H_1)}{p(Y_k(i,j,h)|H_0)} \underset{H_0}{\overset{H_1}{\gtrless}} \gamma$, where γ is the likelihood ratio threshold which can be found by e.g. using the Neyman-Pearson lemma [4], for a preset false-alarm rate P_{fa}.

3. AN ITERATIVE DETECTION APPROACH

The problem of using the Neyman-Pearson test for target detection is the need for having accurate estimates of the parameters of the conditional pdf's under both hypotheses. As demonstrated in [5], the image statistics may vary dramatically, even within a simple scene. Usually, this problem is addressed by using constant false-alarm rate (CFAR) detectors, e.g. order statistics CFAR (OSCFAR) detectors [6].

Here, we present a different approach: An iterative detection scheme which aims at separating target and noise data to obtain the image statistics, instead of blindly using all data within a reference window as done by classical CFAR detectors. We follow the iterative scheme suggested in [5], but use image processing tools for improving the separation of target and noise data. Herein, we do not make any assumption about the statistics of $u_k(i,j,h)$ or $s(i,j,h)$ as we did in [5]. The iterative scheme is depicted in Figure 2. For simplicity, it will be explained using one specific 2D image $Y_{k_0}(i,j,h_0), i = 0,...,I-1, j = 0,...,J-1$ which in the following will be denoted as Y.

Given a false-alarm rate P_{fa} and initial parameters of the conditional pdf's $\hat{\theta}^{H_0,I}$ and $\hat{\theta}^{H_1,I}$ a detection scheme $\mathcal{L}(\cdot)$ (e.g. a Neyman-Pearson test) can be applied, yielding a binary image B^{NP}. This image is then processed by an operator $\mathcal{V}(\cdot)$ which aims at removing outliers and grouping target regions. The resulting image is considered as a first, rough indication of target locations and noise/clutter locations. Based on a division of target samples and noise/clutter samples, parameter estimation can be performed to obtain revised estimates $\hat{\theta}^{H_0}$ and $\hat{\theta}^{H_1}$. The new parameter estimates can again be forwarded to the detector in order to obtain a revised binary image. The iterative detection scheme stops when convergence is achieved which can e.g. be observed by a vanishing difference between subsequent parameter estimates.

The suitability of the iterative framework is particularly dependent on the features of its image processing step. It is, therefore, important to accurately formulate the nominal operation $\mathcal{V}(\cdot)$ for this step. The objective is an accurate pixel-wise division of a normalized B-scan image into a target set

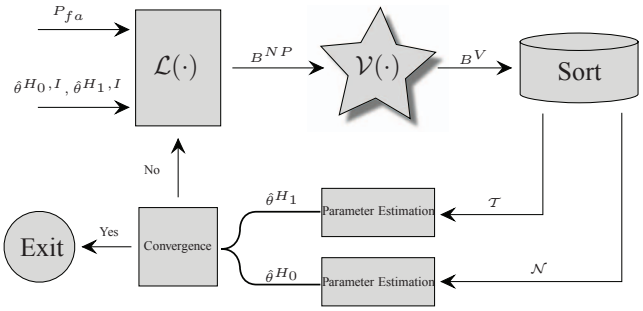

Fig. 2. Iterative Framework

$\mathcal{T}$, comprising of all target samples and its complement, the noise set $\mathcal{N}$, consisting of all noise samples.

B^{NP} can be considered the first rough estimation of the true binary target imaging representation B. The difference between B and B^{NP} stems from false alarms and missed detections (type I and type II errors) immanent when conducting a Neyman-Pearson test. Thus,

$$B^{NP} = B + B_D - B_T \tag{3}$$

The additive term B_D will be referred to as the distorting image (representing all false-alarms) and the subtractive term B_T will be referred to as the truncating image (representing all missed detections). Taking this into consideration, the goal of the operator $\mathcal{V}(\cdot)$ is the accurate estimation of the distorting and truncating set and their subsequent respective elimination and incorporation such that

$$\mathcal{V}[B^{NP}] = B^{NP} - \hat{B}_D + \hat{B}_T \approx B \tag{4}$$

The main contribution of this paper is to derive adequate image processing tools fulfilling the requirement on the operator $\mathcal{V}(\cdot)$ postulated in Equation (4).

4. USING 2D MEDIAN FILTERING

A simple way of processing the binary image B^{NP} is to use 2D median filters as operator $\mathcal{V}(\cdot)$. The filter removes outliers (which are due to type I errors) and extends larger target regions (and thus combats type II errors). The window size has to be chosen empirically, e.g. by considering the smallest object that can be subject to median filter processing.

5. USING MORPHOLOGICAL IMAGE PROCESSING

We propose morphological image processing as a method for providing the distorting and truncating images ($\hat{B}_D$ and $\hat{B}_T$ respectively). The basic morphological dilation and erosion operations [7] $B \oplus E$ and $B \ominus E$ are used for this purpose, where E is the so called structuring element.

A morphological opening, defined by an erosion followed by a dilation operation, is employed to eliminate the distorting

set $\hat{B}_D$ as required by Equation (4). Hereby, it is assumed that the binary set B^{NP} comprises of noise and target objects, which can be defined as spatially isolated pixel groups $B^{NP} = \sum_{n=1}^{N} O_n^{NP}$ with O_n^{NP} being the n^{th} object in B^{NP} and N being the total number of objects in the Neyman-Pearson image. Furthermore B_D can be identified as the sum of all noise objects in B^{NP}. Assuming that the spatial extend of the noise objects in B^{NP} is small in relation to the target objects, we can derive and eliminate B_D from the Neyman-Pearson image B^{NP} by applying morphological opening with an adequate structuring element E_D:

$$B^{NP} \circ E_D = \sum_{n=1}^{N} (O_n^{NP} \ominus E_D) \oplus E_D \quad (5)$$

$$O_n^{NP} \circ E_D = \emptyset \,, \forall n \text{ where } E_D \not\subseteq O_n^{NP} \quad (6)$$

$$O_n^{NP} \circ E_D \approx O_n^{NP} \,, \forall n \text{ where } E_D \subseteq O_n^{NP} \quad (7)$$

$$B_D = \sum_{p \in P} O_p^{NP}; P := \left\{ n \mid E_D \not\subseteq O_n^{NP} \right\} \quad (8)$$

$$B^{NP} \circ E_D = (B^{NP} \ominus E_D) \oplus E_D \approx B^{NP} - B_D \quad (9)$$

Equations (6) and (7) disclose the required specifications for an adequate structuring element E_D. Accordingly the structuring element must be smaller than the smallest target object and larger than the largest noise object.

The estimation of the truncating image B_T can be accomplished via a dilation operation with an adequate structuring element E_T. It is assumed that the target objects in B^{NP} are incomplete, since pixels at the edges of these objects may exhibit lower amplitudes than the threshold γ. Typically one can observe a correlated pixel intensity fading from the center of a target object towards its edge. A morphological dilation would enlarge each target object in order to encompass the target pixels located at the edges of the object. For our purpose, a simple dilation by one pixel is sufficient. The added pixels make up the truncating image,

$$B_T \approx \left[\left(B^{NP} - B_D \right) \oplus E_T \right] - \left(B^{NP} - B_D \right), \quad (10)$$

and therefore

$$\mathcal{V}(B^{NP}) = \left(B^{NP} \circ E_D \right) \oplus E_T \approx B^{NP} - B_D + B_T. \quad (11)$$

6. OPTIMIZING THE STRUCTURING ELEMENT

The size of the structuring element E_D can be designed based on empirical values, e.g. by considering the smallest object to be detected. Additionally, the structuring element can be indirectly optimized by the detection of non-comprehensive estimates for B_D and B_T. Using an optimization algorithm, insufficient estimates of B_D and B_T will elicit detectable truncating and distorting effects. Equations (4) and (11) can be used to find the structuring elements which minimizes these effects, e.g.

$$\hat{E}_D = \arg\max_{E_D} p(\mathcal{N}, \mathcal{T} | E_D). \quad (12)$$

where $p(\mathcal{N}, \mathcal{T}|E_D)$ can be obtained based on knowledge of the image statistics (e.g. Weibull distributed clutter, Gaussian distributed target). In other words, we aim at finding the structuring element which is most likely to produce target and noise sets $\mathcal{N}$ and $\mathcal{T}$ in agreement with the postulated target and noise distribution functions.

The iterative approach from Section 3 can thus be used with various structuring elements $E_D^1, ..., E_D^L$ to obtain $p(\mathcal{N}, \mathcal{T}|E_D^1), ..., p(\mathcal{N}, \mathcal{T}|E_D^L)$ from which one can choose $\hat{E}_D = \arg\max_{E_D^l} p(\mathcal{N}, \mathcal{T}|E_D^l)$.

7. EXPERIMENTAL RESULTS

We considered the same setup as in [5], i.e. the room, depicted in Figure 3(a), consisting of a table, a chair, a metal sphere and a metal dihedral. This scene which lies behind a concrete wall is illuminated from two sides, using the synthetic aperture wideband TTW beamformer presented in [3]. We assumed known wall parameters and background subtracted images. A typical B-Scan image (crossrange vs. downrange 3D cut) is depicted in Figure 3(b). The four table legs can be seen in the lower left quarter, as well as strong noise and clutter contributions. In [5], a truncated Rayleigh model was used to describe $p(Y_k(i,j,h)|H_0)$ whereas $p(Y_k(i,j,h)|H_1)$ was described using a truncated Gaussian distribution. In this paper, we extend the noise model by using a Weibull distribution which allows for more flexibility. All 3D detection results are produced without assuming a priori knowledge of the distribution parameters.

Figures 4(a) and (b) show the results when using the iterative approach presented in Section 3, with a 3×3 median filter and morphological operations for 60 B-Scans starting from the floor to the top of the metal dihedral in steps of 1in. Typically, convergence is achieved after $3-4$ iterations. The false-alarm rate is fixed at 0.7%. When using the morphological operations, the structuring element E_D is optimized for every height, using the algorithm presented in Section 6 only for circular elements. It can be seen that although the median filter yields a cleaner binary image, important details such as part of the table (indicated by a red ellipse) and the metal sphere are missing. The dihedral (green dashed ellipse) can clearly be detected. When using morphological operations, all four table legs are present as well as the dihedral and the metal sphere (yellow dash-dotted ellipse). However, this comes at the cost of increased clutter.

For comparison, the OSCFAR detector presented in [6] is shown in Figure 4(c). As suggested by Levanon and Shor [8], the 16.7th and 97.3rd percentile have been used to estimate the shape parameter of the Weibull distribution. This

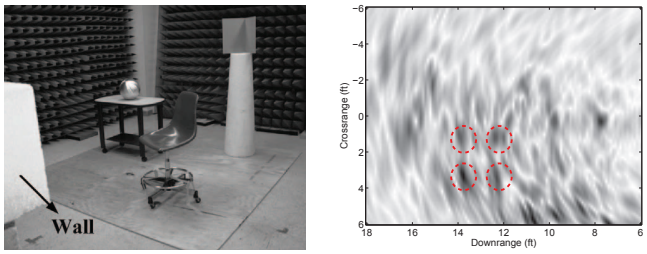

(a) 3D scene of interest (b) Typical B-scan image

Fig. 3. Experimental setup

detector offers less image details compared to the median filter approach. The table legs cannot be detected and the metal sphere is missing.

8. CONCLUSIONS

An iterative scheme for target detection in Through-the-wall Radar Imaging has been presented. This scheme adapts itself to the unknown image statistics and is able to perform automatic 3D detection. It has successfully been evaluated using experimental data and showed improved detection performance when compared with an order statistics CFAR detector.

9. REFERENCES

[1] E. Baranoski, "Through wall imaging: Historical perspective and future directions," in *Proc. of the 3rd IEEE International Conference on Acoustics, Speech and Signal Processing*, 2008.

[2] L.-P. Song, C. Yu, and Q. H. Liu, "Through-wall imaging (twi) by radar: 2-D tomographic results and analyses," *IEEE Transactions on Geoscience and Remote Sensing*, vol. 43, no. 12, pp. 2793–2798, 2005.

[3] F. Ahmad and M. G. Amin, "Wideband synthetic aperture imaging for urban sensing applications," *Journal of the Franklin Institute*, vol. 345, no. 6, pp. 618–639, September 2008.

[4] S. M. Kay, *Fundamentals of Statistical Signal Processing, Volume 2: Detection Theory*, Prentice Hall PTR, 1998.

[5] C. Debes, M.G. Amin, and A.M. Zoubir, "Target detection in single- and multiple-view through-the-wall radar imaging," *IEEE Transactions on Geoscience and Remote Sensing, To appear*.

[6] P. Weber and S. Haykin, "Ordered statistic CFAR processing for two-parameter distributions with variable skewness," *IEEE Transactions on Aerospace and Electronic Systems*, vol. AES-21, no. 6, pp. 819–821, 1985.

[7] R.C. Gonzales and R.E. Woods, *Digital Image Processing*, Prentice Hall, 2001.

[8] N. Levanon and M. Shor, "Order statistics CFAR for weibull background," *IEE Proceedings on Radar and Signal Processing*, vol. 137, no. 3, pp. 157–162, 1990.

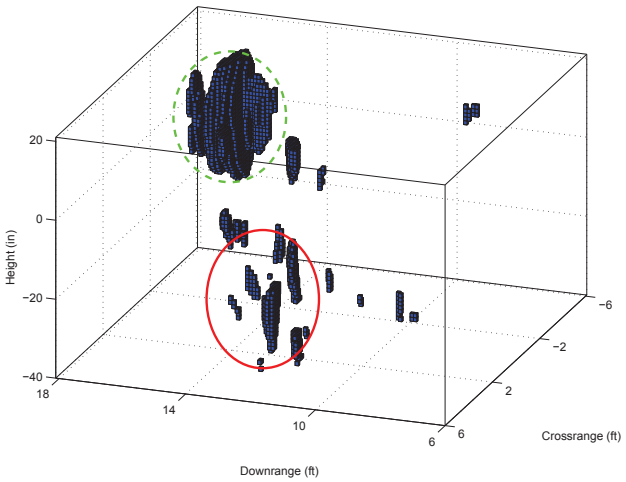

(a) Iterative approach using Median Filtering

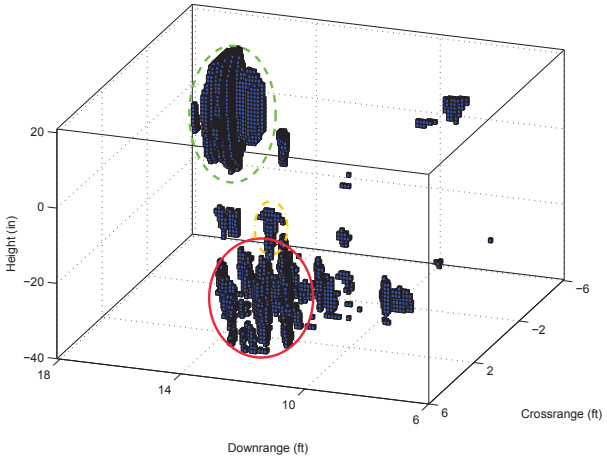

(b) Iterative approach using Morphological Operations

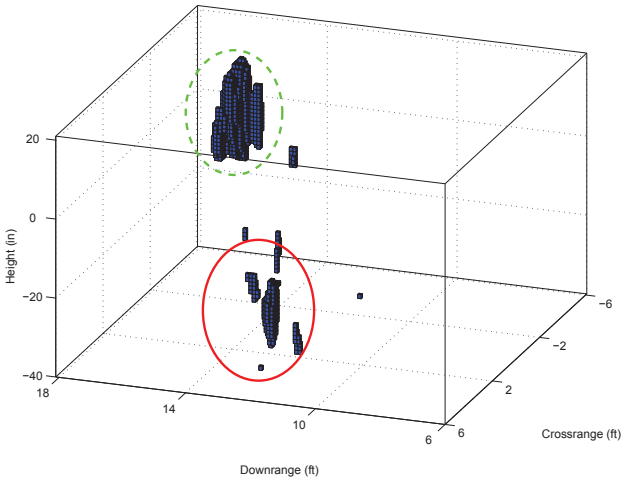

(c) Order statistics CFAR

Fig. 4. 3D Detection Results